Carcinogenesis vol.33 no.9 pp.1814–1821, 2012
doi:10.1093/carcin/bgs234
Advance Access Publication July 12, 2012

Identification of mammalian target of rapamycin as a direct target of fenretinide both *in vitro* and *in vivo*

Hua Xie†, Feng Zhu†, Zunnan Huang, Mee-Hyun Lee, Dong Joon Kim, Xiang Li, Do Young Lim, Sung Keun Jung, Soouk Kang, Haitao Li, Kanamata Reddy, Lei Wang, Weiya Ma, Ronald A.Lubet[1], Ann M.Bode and Zigang Dong*

The Hormel Institute, University of Minnesota, Austin, Minnesota, USA and [1]National Institutes of Health, National Cancer Institute, MD, USA

*To whom correspondence should be addressed. The Hormel Institute, University of Minnesota, 801 16th Avenue NE, Austin, MN 55912-3679. Tel: +507 437 9600; Fax: +507 437 9606;Email: zgdong@hi.umn.edu

***N*-(4-hydroxyphenyl) retinamide (4HPR, fenretinide) is a synthetic retinoid that has been tested in clinical trials as a cancer therapeutic and chemopreventive agent. Although 4HPR has been shown to be cytotoxic to many kinds of cancer cells, the underlying molecular mechanisms are only partially understood. Until now, no direct cancer-related molecular target has been reported to be involved in the antitumor activities of 4HPR. Herein, we found that 4HPR inhibited mammalian target of rapamycin (mTOR) kinase activity by directly binding with mTOR, which suppressed the activities of both the mTORC1 and the mTORC2 complexes. The predicted binding mode of 4HPR with mTOR was based on a homology computer model, which showed that 4HPR could bind in the ATP-binding pocket of the mTOR protein through hydrogen bonds and hydrophobic interactions. *In vitro* studies also showed that 4HPR attenuated mTOR downstream signaling in a panel of non-small-cell lung cancer cells, resulting in growth inhibition. Moreover, knockdown of mTOR in cancer cells decreased their sensitivity to 4HPR. Results of an *in vivo* study demonstrated that i.p. injection of 4HPR in A549 lung tumor-bearing mice effectively suppressed cancer growth. The expression of mTOR downstream signaling molecules in tumor tissues was also decreased after 4HPR treatment. Taken together, our results are the first to identify mTOR as a direct antitumor target of 4HPR both *in vitro* and *in vivo*, providing a valuable rationale for guiding the clinical uses of 4HPR.**

Introduction

N-(4-hydroxyphenyl) retinamide (4HPR), also known as fenretinib, is a synthetic retinoid that has been widely tested in clinical trials as a cancer therapeutic and chemopreventive agent (1). 4HPR has been shown to inhibit carcinogenesis in a variety of cancer cells, including breast cancer (2), bladder cancer (3), lung cancer (4), prostate cancer (5) and leukemia (6–7). Clinical trials have shown that 4HPR induces a significant reduction of secondary breast cancers in premenopausal women (8). However, the mechanisms of the antitumor activity of 4HPR have not been fully elucidated. Previous studies demonstrated that induction of apoptosis is a key mechanism of 4HPR to inhibit tumor growth. 4HPR could induce apoptosis of cancer cells both in retinoic acid receptor-dependent and -independent manners (9–10). The activation of c-Jun *N*-terminal kinases and the mitochondrial apoptotic pathway through the generation of reactive oxygen species was reported to be involved in 4HPR-induced apoptosis (11–12). Moreover, studies also showed that anti-angiogenic effects mediated through vascular endothelial growth factor receptor (VEGFR) (13–14) and inhibition of tumor invasion by interfering with Matrix metalloproteinase (MMP) (15–16) also underlie the antitumor activity of 4HPR. Several molecules in different signaling transduction pathways, such as FAK/Akt/GSK3β, have also been reported to be involved in the antitumor activity of 4HPR (5,17). Recently, Rahmaniyan and colleagues identified dihydroceramide desaturase, an enzyme that is responsible for inserting the 4,5-trans-double bond into the sphingolipid backbone of dihydroceramide, as a direct *in vitro* target of 4HPR (18). However, a direct antitumor target of 4HPR has not yet been identified in cells or *in vivo*.

The mammalian target of rapamycin (mTOR) is a major component of the PI3-K/Akt/mTOR pathway. It is an evolutionarily conserved serine/threonine kinase and functions as a sensor of mitogen, energy and nutrient levels and is a central controller of cell growth and division (19). The PI3-K/Akt/mTOR pathway is deregulated in 50% of all human malignancies, and therefore, inhibition of mTOR is a promising strategy for the treatment of human cancers. mTOR has two functionally distinct multi-protein complexes, mTOR complex 1 (mTORC1) and mTORC2. mTORC1 contains Raptor and PRAS40 and regulates protein translation through phosphorylation of p70 ribosomal S6 kinase (p70S6K) and eukaryotic translation initiation factor binding protein (4E-BP) (20). mTORC2 contains Rictor and Protor and phosphorylates Akt on Ser473, thereby increasing Akt enzymatic activity (21–22). mTOR inhibitors are currently being developed as potential antitumor agents. Rapamycin and its derivatives (referred to as rapalogs) are the most well-characterized mTOR inhibitors. The rapamycins are allosteric inhibitors that, in complex with FKBP12, target the FKB domain of mTOR (23). They partially inhibit mTOR through allosteric binding to mTORC1, but not mTORC2 (24). However, inhibiting only mTORC1 may not be sufficient for achieving a broad and robust anticancer effect due to a failure to inhibit mTORC2 in some tumor types. A strong interest now exists in developing small-molecule mTOR kinase inhibitors, which target both mTORC1 and mTORC2.

In the present study, we report for the first time that mTOR is a direct antitumor target of 4HPR. 4HPR effectively targets both mTORC1 and mTORC2 by directly binding to mTOR, resulting in the inhibition of tumor growth both in cells and *in vivo*.

Abbreviations: 4HPR, N-(4-hydroxyphenyl) retinamide; mTOR, mammalian target of rapamycin; H&E, hematoxylin and eosin.

†These authors contributed equally to this work.

Materials and methods

Reagents and antibodies

4HPR was obtained from the National Institutes of Health (NIH). Rapamycin was purchased from LC Laboratories (Woburn, MA). Recombinant active mTOR (1362-end) was purchased from Millipore (Billerica, MA). The inactive p70S6K protein was from SignalChem (Richmond, BC, CANADA) and CNBr-Sepharose 4B was purchased from GE Healthcare (Pittsburgh, PA).

Cell culture and transfection

All cell lines were purchased from American Type Culture Collection and were cultured in monolayers at 37°C in a 5% CO_2 incubator according to American Type Culture Collection protocols. For transfection experiments, the jetPEI (Qbiogen, Inc.) transfection reagent was used following the manufacturer's instructions.

Anchorage-independent cell transformation assay

Tumor cells were suspended in Basal Medium Eagle medium and added to 0.6% agar, with different concentrations of 4HPR in a base layer and a top layer of 0.3 % agar. For JB6 Cl41 cells, the procedure is similar, except that these cells were exposed to Epidermal growth factor (EGF) (20 ng/ml) during treatment with 4HPR or vehicle. The cultures were maintained at 37°C in a 5% CO_2 incubator for 1–2 weeks and then colonies were counted under a microscope using the Image-Pro Plus software (v.4) program (Media Cybernetics, Silver Spring, MD).

MTS assay

To estimate cytotoxicity, cells were seeded (8×10^3 cells per well) in 96-well plates and cultured overnight. Cells were then fed with fresh medium and treated with different doses of 4HPR. After culturing for various times, the cytotoxicity of 4HPR was measured using an MTS (3-(4,5-dimethylthiazol-2-yl)-5-(3-carboxymethoxyphenyl)-2H-tetrazdium) assay kit (Promega, Madison, WI) according to the manufacturer's instructions.

Computational modeling

The three-dimensional structure of mTOR was obtained from the SWISS-MODEL Repository, which is a homology model based on the crystal structure of PI3K-delta (PDB id 2WXG). Protein–ligand docking was performed using the high-performance hierarchical docking algorithm, Glide. The final binding model structure of mTOR-4HPR was generated from Schrodinger Induced Fit Docking, which merges the predictive power of prime with the docking and scoring capabilities of Glide for accommodating the possible protein conformational change upon ligand binding.

Western blot analysis

Proteins were resolved by sodium dodecyl sulfate–polyacrylamide gel electrophoresis and transferred onto polyvinylidene difluoride membranes (Millipore, Billerica, MA), which were blocked with milk and hybridized with specific primary antibodies. The protein bands were visualized using an enhanced chemiluminescence reagent (GE Healthcare, Pittsburgh, PA) after hybridization with a horseradish peroxidase-conjugated secondary antibody.

mTOR in vitro kinase assay

Inactive p70S6K (1 µg) or inactive Akt1 (1 µg) proteins were used as the substrate, respectively, for an *in vitro* kinase assay with 250 ng of active mTOR (1362-end). Reactions were carried out in 1 × kinase buffer (25 mM Tris-HCl pH 7.5, 5 mM beta-glycerophosphate, 2 mM dithiothreitol, 0.1 mM Na_3VO_4, 10 mM $MgCl_2$ and 5 mM $MnCl_2$) containing 100 µM ATP at 30°C for 30 min. Reactions were stopped and proteins detected by western blotting.

Immunoprecipitation and detection of mTOR complexes

The mTOR complexes mTORC1 and mTORC2 were immunoprecipitated with a polyclonal rictor or polyclonal raptor antibody, followed by western blotting to detect mTOR and raptor or rictor, as described previously (25).

In vitro pull-down assay

Recombinant human mTOR (1362-end) (200 ng) or cell lysates (1 mg) were incubated with 4HPR-Sepharose 4B beads (or Sepharose 4B beads alone as a control) (100 µl, 50% slurry) in the reaction buffer [50 mM Tris (pH 7.5), 5 mM ethylenediaminetetraacetic acid, 150 mM NaCl, 1 mM dithiothreitol, 0.01% Nonidet P-40, 2 µg/ml bovine serum albumin, 0.02 mM phenylmethylsulfonyl fluoride and 1 µg/ml protease inhibitor mixture]. After incubation with gentle rocking overnight at 4°C, the beads were washed five times and proteins bound to the beads were analyzed using western blotting.

Xenograft mouse model

Athymic nude mice [Cr:NIH (S), NIH Swiss nude, 6- to 9-week old] were obtained from Harlan Laboratories and maintained under 'specific pathogen-free' conditions based on the guidelines established by the University of Minnesota Institutional Animal Care and Use Committee. Mice were divided into different groups ($n = 10$ of each group). A549 lung cancer cells (4×10^6/0.1 ml) were injected subcutaneously into the right flank of each mouse. 4HPR was freshly prepared once a week and protected from light and kept at 4°C as described previously (26–27). 4HPR or vehicle was administered by i.p. injection three times a week for 29 days. Tumor volumes and body weights were measured. Tumor tissues from mice were embedded in a paraffin block and subjected to immunohistochemistry or hematoxylin and eosin (H&E) staining.

Statistical analysis

All quantitative data are expressed as mean values ± standard deviation, and significant differences were determined by Student's t test or by one-way ANOVA. A probability value of $P < 0.05$ was used as the criterion for statistical significance.

Results

4HPR inhibits EGF-induced neoplastic transformation and signal transduction in JB6 Cl41 cells

In the present study, we first examined the effect of 4HPR (Figure 1A) on EGF-induced neoplastic transformation of JB6 Cl41 cells. Treatment of JB6 Cl41 cells with 4HPR significantly inhibited EGF-promoted neoplastic transformation in a dose-dependent manner (Figure 1B). 4HPR at 10 or 20 µM caused a decrease to 46 or 89% of control, respectively. The inhibition of colony formation by 4HPR was not due to cytotoxicity because the effective concentration range for suppressing cell transformation did not affect JB6 Cl41 cell viability (Figure 1C). Because anchorage-independent growth ability is an *ex vivo* indicator and a key characteristic of the transformed cell phenotype (28), these results suggest that 4HPR can reduce the malignant potential of JB6 Cl41 cells induced by EGF.

To identify a potential target of 4HPR, we examined several key-signaling molecules, including those in the RAS/RAF/MEK and PI3-K/Akt/mTOR pathways, which are frequently deregulated in human malignancies. Western blot results showed that 4HPR suppressed the phosphorylation of p70S6K and S6 ribosomal protein (S6) in a dose-dependent manner (Figure 1D) but had no inhibitory effect on the phosphorylation of other molecules, including EGFR, RAF, MEK and ERKs (data not shown).

4HPR is a potent inhibitor of mTOR kinase activity

The above results showed that the phosphorylation of p70S6K (T389), a direct downstream target of the PI3-K/Akt/mTOR pathway, was inhibited after 4HPR treatment, indicating that upstream molecules, such as PI3-K, Akt and mTOR, might be important targets of 4HPR. To this end, we first examined the effects of 4HPR on Akt1/2 or PI3-Kα/β *in vitro* kinase activity, but only weak inhibition was observed even at the highest concentration of 4HPR (20 µM) (data not shown). This raised the possibility that mTOR might be an important target of 4HPR. We performed an *in vitro* kinase assay with recombinant mTOR in the presence of various concentrations of 4HPR without FKBP12. Wortmannin, a well-known inhibitor of both PI3-K and mTOR, was used as a positive control in this assay. The phosphorylation of p70S6K (Thr389), an mTOR substrate, was strongly inhibited by 4HPR in a concentration-dependent manner (Figure 2A). For example, 1 µM 4HPR caused a 43% inhibition of mTOR kinase activity and 20 µM 4HPR resulted in an 88% inhibition. Moreover, we also used inactive Akt1 as a substrate for mTOR and results indicated that the phosphorylation of Akt on Ser473 was also dose-dependently suppressed by 4HPR treatment (Figure 2B). These results clearly support our hypothesis that mTOR is a direct target of 4HPR and, notably, the activity of both mTORC1 and mTORC2 might be inhibited by 4HPR.

4HPR directly binds with mTOR

We then constructed a possible binding model of 4HPR with the mTOR protein using molecular docking. The three-dimensional structure of mTOR was obtained from the SWISS-MODEL Repository (29). The model is a homology model based on the crystal structure of PI3K-delta (PDB id 2WXG) (30). The binding pose of 4HPR-mTOR obtained from the docking result (Figure 2C) suggested that the binding of 4HPR to mTOR extended from the ATP site into the neighboring hydrophobic pocket. 4HPR formed three hydrogen bonds with the protein residues in the ATP-binding pocket—two with Ser2165 and the other with Lys2187. In addition, several residues, including Tyr2225, Val2240, Met2345, Leu2354 and Ile2356 showed strong hydrophobic interactions with the major retinal part of 4HPR.

The docking results indicated that 4HPR formed a good interaction with the mTOR active site, which might be the basis of the direct binding of 4HPR to mTOR. To confirm this idea, we performed an *in vitro* binding assay using 4HPR-conjugated Sepharose 4B beads or control Sepharose 4B beads. No obvious band was observed when the mTOR protein was incubated with Sepharose 4B beads, whereas a strong band was seen when mTOR was incubated with 4HPR-conjugated Sepharose 4B beads (Figure 2D), clearly indicating that 4HPR directly binds to recombinant mTOR. We then performed an *ex vivo* pull-down assay using A549 cells, and similar results were also obtained with an A549 lung cancer cell lysate (Figure 2E). Therefore, these results indicated that 4HPR binds directly to mTOR and inhibits mTOR kinase activity.

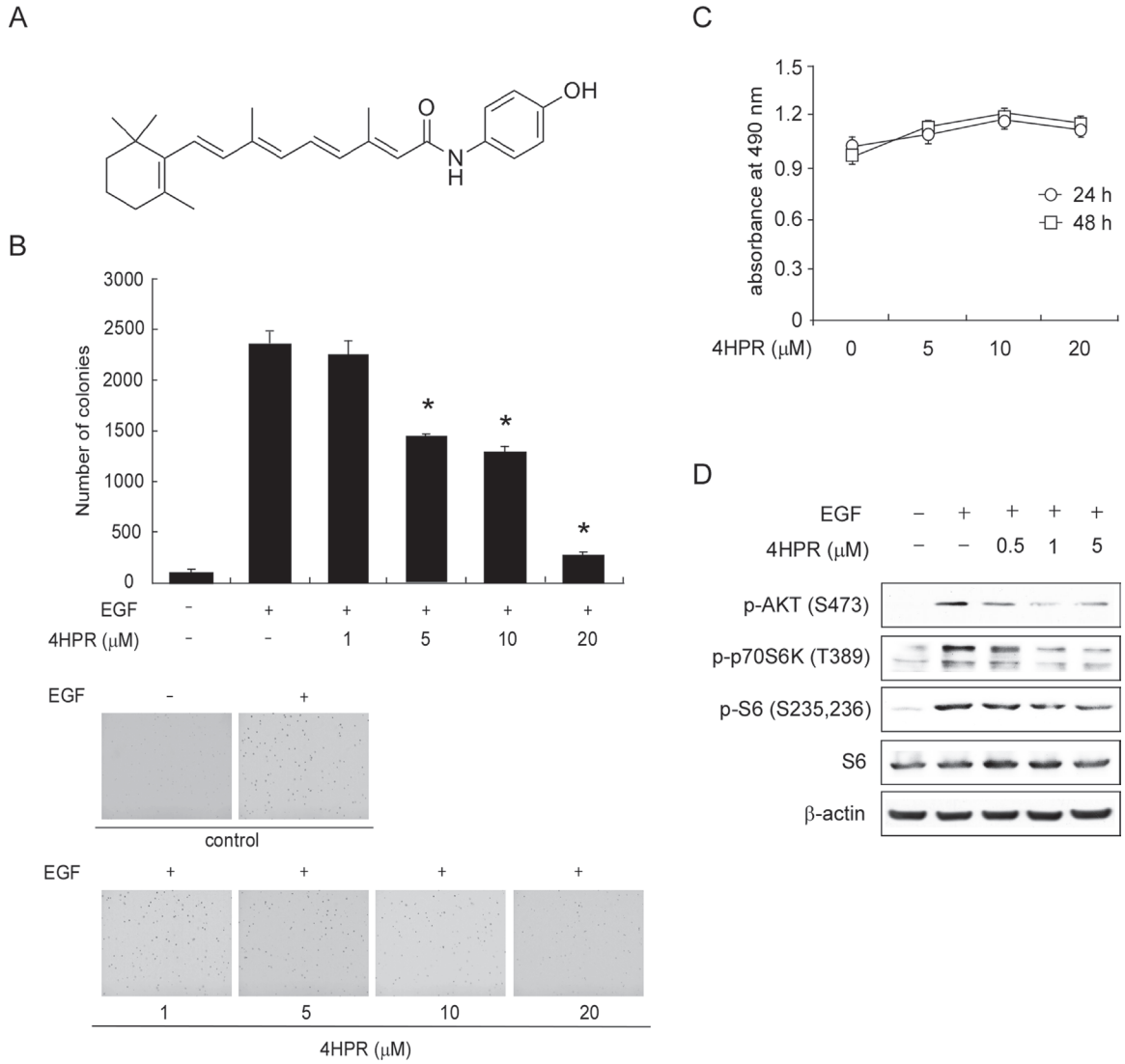

Fig. 1. Chemical structure of 4HPR and its effect on EGF-induced neoplastic transformation and signal transduction in JB6 Cl41 cells. (**A**) Chemical structure of 4HPR. (**B**) 4HPR inhibits EGF-induced anchorage-independent growth of JB6 Cl41 cells. Data are shown as means ± standard deviation of values from three independent experiments and the asterisk indicates a significant (*$P < 0.01$) decrease in colony formation in cells treated with 4HPR compared with the DMSO-treated group. (**C**) Cytotoxic effects of 4HPR on JB6 Cl41 cells. An MTS assay was used after treatment of cells with 4HPR for 24 or 48 h, respectively. (**D**) 4HPR inhibits signal transduction in JB6 Cl41 cells. After starvation in serum-free medium for 24 h, cells were treated with 4HPR at the indicated concentration for 2 h and then stimulated with EGF (20 ng/ml) for 15 min. Cells were then harvested and protein levels were determined by western blot analysis.

4HPR inhibits downstream targets of both mTORC1 and mTORC2 in human lung cancer cells and suppresses cell growth

Previous studies suggested that the mTOR signaling pathway is highly activated in human lung cancer (31–34). Therefore, we examined the effect of 4HPR in a panel of non-small-cell lung cancer cells. First, we investigated the effects of 4HPR on anchorage-independent growth of different types of human lung cancer cells. The results showed that 4HPR significantly inhibited A549 cell growth in soft agar in a concentration-dependent manner (Figure 3A). Colony formation was inhibited by more than 30% after treatment with 4HPR at a concentration of 5 μM, and almost no colonies were formed at 20 μM (Figure 3A). Moreover, we also examined the effect of 4HPR on the growth of several other lung cancer cell lines, including H520, H1650 and HCC827. Results showed that 4HPR dose dependently inhibited the growth of each cell line on soft agar (Figure 3B–3D).

We then investigated the effect of 4HPR on downstream targets of mTOR, including the phosphorylation of p70S6K and S6, as well as phosphorylation of Akt, in both A549 cells and H520 cells, which were relatively more sensitive to 4HPR (Figure 3A–3D). Western blot results showed that in both of the cell lines, mTOR-mediated phosphorylation of p70S6K (T389), S6 (S235, 236), as well as Akt (S473), was substantially decreased dose dependently with 4HPR treatment (Figures 3E and 3F).

4HPR inhibits both mTORC1 and mTORC2

Next, we determined the effect of 4HPR on mTORC1 and mTORC2 complexes using immunoprecipitation. Results indicate that both raptor (Figure 4A) and rictor (Figure 4B), members of the mTORC1 and mTORC2 complexes, were decreased with 4HPR treatment in A549 cells. In contrast, the control compound rapamycin only suppressed raptor in mTORC1 but not rictor in mTORC2 at a concentration of 10 nM, which is consistent with a previous report (24). These results indicated that 4HPR can target both the mTORC1 and mTORC2 complexes.

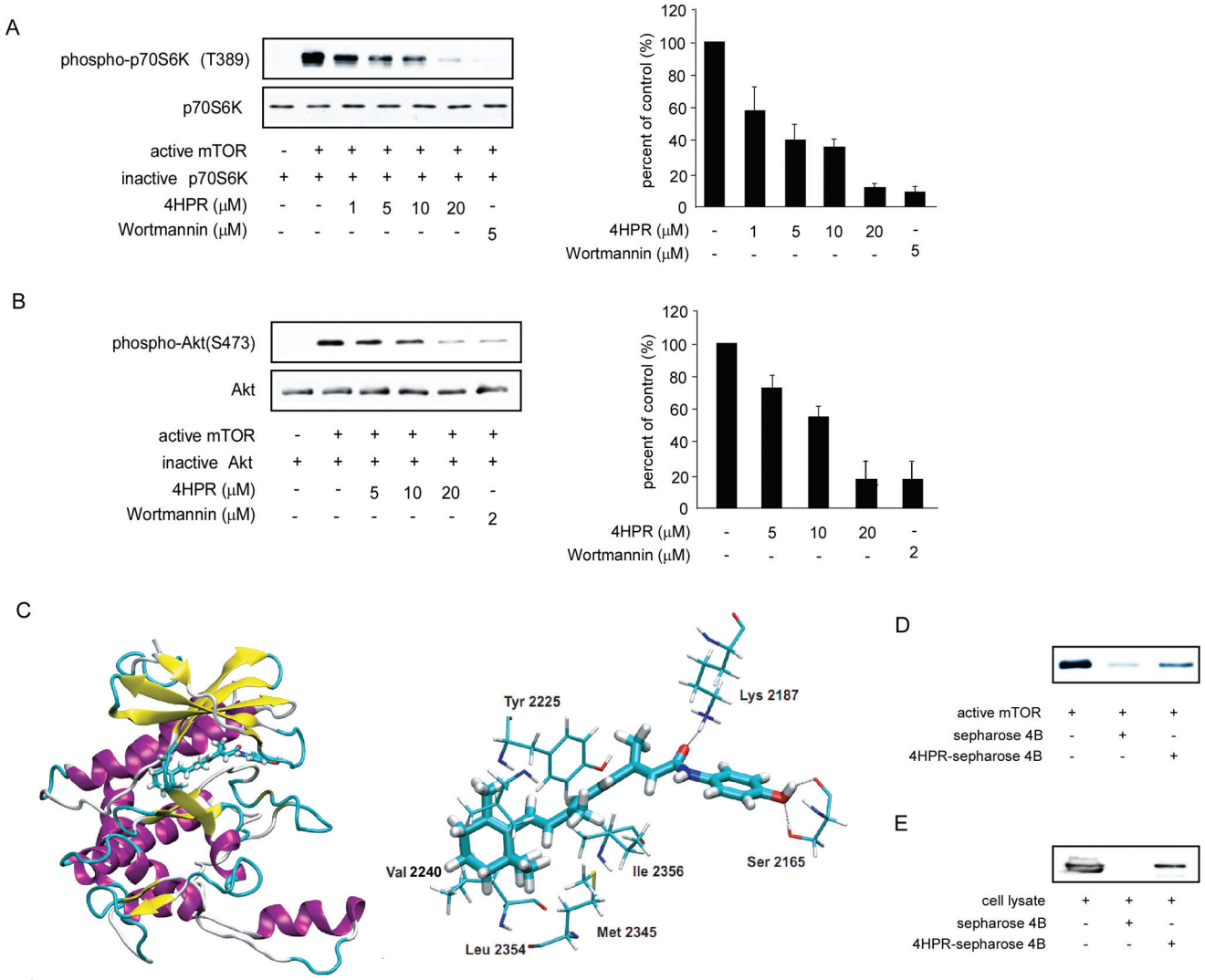

Fig. 2. 4HPR inhibits mTOR kinase activity by directly binding with mTOR. A, 4HPR inhibits mTOR *in vitro* kinase activity in a concentration-dependent manner. An inactive p70S6K (**A**) or inactive Akt1 protein (**B**) was used as the substrate, respectively, for *in vitro* kinase assays with active mTOR and 100 μM ATP. Proteins were resolved by sodium dodecyl sulfate–polyacrylamide gel electrophoresis and detected by western blotting. (**C**) proposed binding model of 4HPR-mTOR. 4HPR is shown in stick model and protein residues are shown in line model. 4HPR formed hydrogen bonds with Ser2165 and Lys2187. Several residues, including Tyr2225, Val2240, Met2345, Leu2354 and Ile2356 displayed strong hydrophobic interactions with the major retinal part of 4HPR. The figures were generated with VMD and Maestro. (**D** and **E**) 4HPR binds directly to mTOR *in vitro* (**D**) and *ex vivo* (**E**). Sepharose 4B was used for binding and pull-down assays as described in section 'Materials and methods'. Lane 1 is input control (mTOR protein standard); lane 2 is the negative control, indicating no binding between mTOR and Sepharose 4B beads; and lane 3 shows that mTOR binds with 4HPR-Sepharose 4B beads.

Knockdown of mTOR in A549 cells decreased the sensitivity of 4HPR

We then examined whether knocking down mTOR expression influences the sensitivity of A549 cancer cells to 4HPR. First, we determined the efficiency of shRNA knockdown, as well as the effect of shRNA transfection on anchorage-independent growth. The expression of mTOR was obviously decreased after shRNA transfection (Figure 5A). Moreover, the growth of cells on soft agar also decreased more than 30% after transfection compared with the mock group (Figure 5B). Next, A549 cells transfected with *mTOR shRNA* or *mock control* were treated with 4HPR or vehicle and subjected to a soft agar assay. The results showed that 4HPR (10 μM) inhibited anchorage-independent growth of A549 cells transfected with *mock shRNA* by about 55%. In contrast, the inhibition was only about 37% in A549 cells transfected with *mTOR shRNA*, indicating that A549 cells transfected with *mTOR shRNA* were more resistant to 4HPR treatment (Figure 5C). These results suggested that mTOR plays an important role in the sensitivity of A549 cells to the antiproliferative effects of 4HPR.

4HPR inhibits growth of lung cancer cells in a xenograft model

To explore the antitumor activity of 4HPR *in vivo*, A549 cancer cells were injected into the right flank of individual athymic nude mice. Mice were then administered vehicle or 4HPR by i.p. injection of 10 or 40 mg/kg three times a week for 29 days. The results showed that treatment of mice with 10 or 40 mg/kg BW of 4HPR significantly suppressed A549 tumor growth by 52 and 73%, respectively, relative to the vehicle-treated group (Figure 6A, $P < 0.01$). Moreover, mice seemed to tolerate treatment with these doses of 4HPR without overt signs of toxicity or significant loss of body weight compared with vehicle-treated group (Figure 6B). The effect of 4HPR on mTOR protein targets was evaluated by immunohistochemistry and H&E

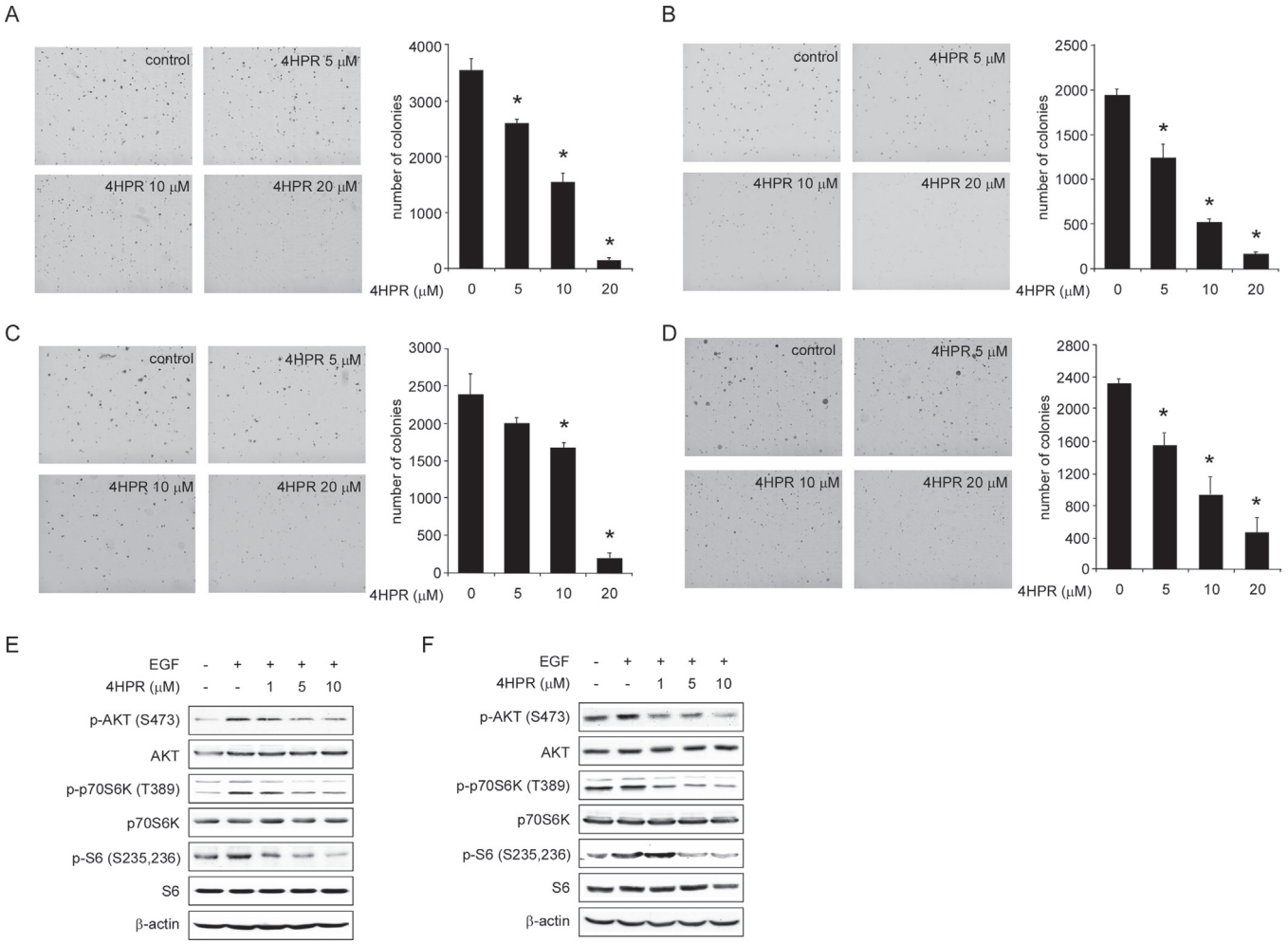

Fig. 3. Effects of 4HPR on anchorage-independent growth and mTOR signaling in lung cancer cells. (**A–D**) 4HPR inhibits anchorage-independent growth in a panel of NSCLC cell lines, including A549 cells (**A**), H520 cells (**B**), H1650 cells (**C**) and HCC827 cells (**D**). Data are shown as means ± standard deviation and the asterisk indicates a significant ($*P < 0.01$) decrease in colony formation in cells treated with 4HPR compared with the dimethyl sulfoxide –treated group. (**E** and **F**) 4HPR inhibits mTOR signaling in A549 cells (**E**) and H520 cells (**F**). Cells were starved in serum-free medium for 24 h, and then treated with 4HPR at the indicated concentration for 2 h. After stimulation with EGF (20 ng/ml) for 15 min, cells were harvested and protein levels were determined by western blot analysis.

staining of A549 tumor tissues after 29 days of treatment. The expression of phosphorylated p70S6K, a direct target of mTOR, was markedly decreased after treatment with 4HPR at either 10 or 40 mg/kg B.W. (Figure 6C and 6D). In addition, the phosphorylation of S6 on S235,236 and the phosphorylation of Akt on S473 in tumor tissues was also strongly suppressed by 4HPR at 10 or 40 mg/kg B.W. (Figure 6E). These data indicated that A549 lung tumor development was suppressed by 4HPR through inhibition of the both the mTORC1 and mTORC2 signaling pathways.

Discussion

4HPR is a highly active and promising therapeutic and chemopreventive agent (1). However, the underlying mechanism explaining its anticancer activity has not yet been elucidated. The present study identified mTOR as a direct target of 4HPR both *in vitro* and *in vivo*.

Previous reports revealed that the PI3-K/Akt/mTOR pathway may be involved in the antitumor activity of 4HPR, and the phosphorylation of Akt (Ser473) is reportedly involved in 4HPR-mediated apoptosis (5,17). Our results indicated that 4HPR effectively suppressed EGF-induced transformation of JB6 Cl41 cells that was accompanied by decreased phosphorylation of Akt (Ser473) and p70S6K (Thr389) (Figure 1D). Thus, the PI3-K/Akt/mTOR pathway is likely to play an important role in the antitumor activity of 4HPR. We first determined whether 4HPR could affect the kinase activity of Akt1/2 or PI3-Kα/β using an *in vitro* kinase assay. However, only a weak inhibition was observed even at the highest concentration (20 μM) (data not shown). These results indicated that Akt and PI3-K are probably not the major or direct targets of 4HPR, because the plasma concentration of 4HPR reportedly ranges from 0.7 to 10 μM at steady state (35). Previous studies have shown that phosphorylated p70S6K (Thr389) and Akt (Ser473) are downstream targets of mTORC1 and mTORC2, respectively (21,36). Therefore, we hypothesized that mTOR, which is located downstream in this pathway, might be an important and potential direct target of 4HPR. Thus, we determined the effect of 4HPR on mTOR *in vitro* kinase activity. Consistent with our idea, the results clearly showed that 4HPR could potently suppress mTOR activity *in vitro* in a concentration-dependent manner. This compound also reduced the phosphorylation of mTOR downstream molecules in cancer cells resulting in the inhibition of

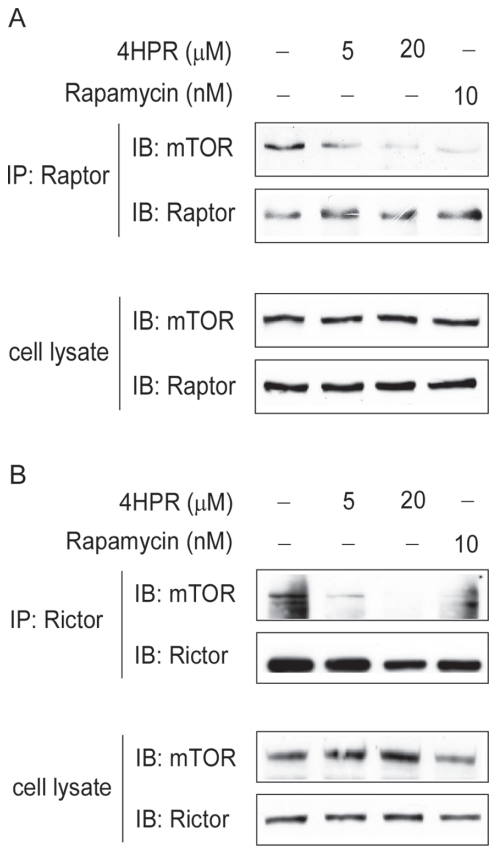

Fig. 4. 4HPR targets both mTORC1 and mTORC2. (**A**) Lysates of A549 cells were subjected to immunoprecipitation using a raptor antibody followed by western blotting using anti-mTOR and antiraptor. (**B**) Lysates of A549 cells were subjected to immunoprecipitation using a rictor antibody followed by western blotting using anti-mTOR and antiraptor.

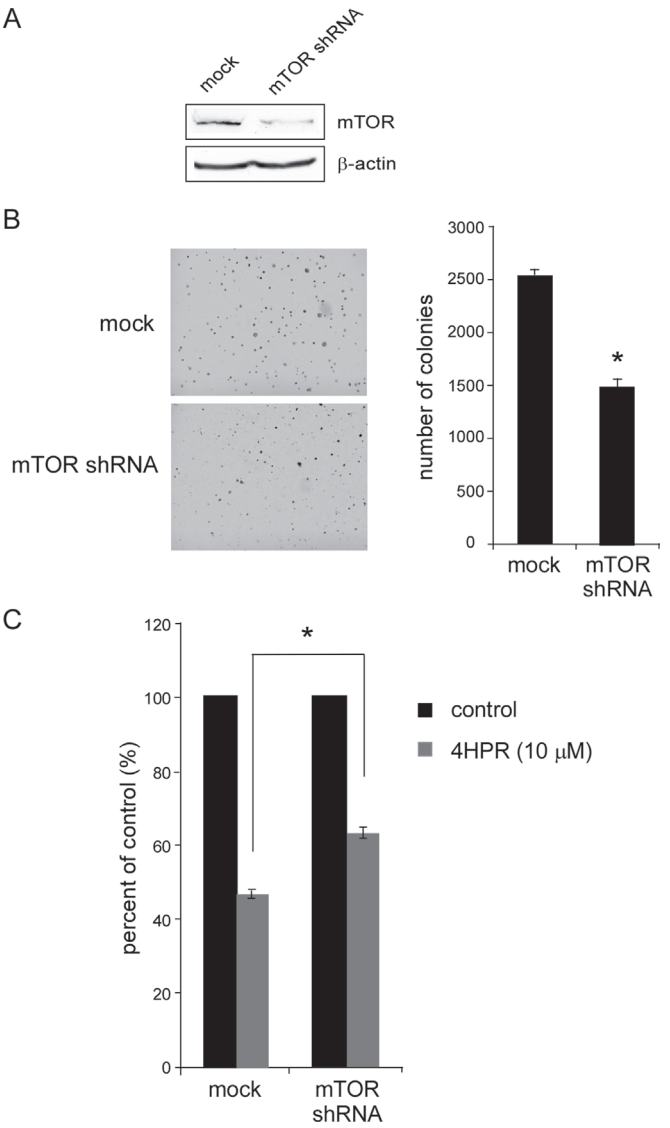

Fig. 5. Knockdown of mTOR in A549 cells decreases sensitivity to 4HPR. (**A**) Efficiency of mTOR shRNA in A549 cells. (**B**) Anchorage-independent growth of A549 cells transfected with *mock shRNA* or *mTOR shRNA*. (**C**) Sensitivity of A549 cells transfected with *mock shRNA* or *mTOR shRNA* to treatment with 4HPR.

growth of several types of human lung cancer cells. In addition, knocking down mTOR expression decreased the sensitivity of A549 cells to 4HPR treatment. Moreover, results of an *in vivo* study using a xenograft mouse model further confirmed that 4HPR inhibited mTOR's protein targets in tumor tissues resulting in inhibition of tumor growth *in vivo*. Overall, these results clearly demonstrated that mTOR is a direct and important antitumor target of 4HPR.

Accumulating studies have demonstrated that apoptosis is a key mechanism of 4HPR antitumor activity. However, in the present study, no obvious apoptosis was observed in JB6 C141 cells and A549 cells after exposure to 4HPR for 48 h at the concentration (20 μM or less) that required for mTOR inhibition and anchorage-independent growth inhibition (data not shown). In addition, we also examined the apoptosis-inducing activity of 4HPR in leukemia cells and breast cancer cells, and results demonstrated that the sensitivity of these cells to 4HPR varied obviously (data not shown). Therefore, these results indicated that 4HPR might induce apoptosis in a cell-line-dependent manner and mTOR might play more important role in the growth inhibitory activity of 4HPR than that in apoptosis induction, at least in the cells tested in the present study. Our molecular docking results showed that 4HPR might bind to the ATP-binding pocket of mTOR through hydrogen bonding with Ser2165 and Lys2187 and hydrophobic interactions with several amino acid residues, including Tyr2225, Val2240, Met2345, Leu2354 and Ile2356. A previous report (37) showed that most of these amino acid residues are important for the binding between mTOR and ATP or mTOR inhibitors. Thus, the predicted binding model between 4HPR and mTOR is very similar to that of other reported mTOR inhibitors. Subsequently, we performed an *in vitro* binding and *ex vivo* pull-down assays to determine whether 4HPR can bind directly with mTOR. The results confirmed the direct binding between 4HPR and the mTOR protein. Therefore, these results demonstrated that 4HPR inhibited mTOR kinase activity through its direct binding to the mTOR protein.

Rapamycin and its analogues have shown that mTOR is an attractive target in cancer. mTORC1 is sensitive to the selective inhibitor, rapamycin, and is activated by growth factor stimulation by the canonical PI3-K/Akt/mTOR pathway. However, mTORC2 is not rapamycin sensitive, mainly due to Akt activation by disruption of a negative feedback loop (38). The negative feedback, which is dependent on IGF1R/insulin receptor substrate 1, involves the S6K-mediated suppression of upstream signaling. mTORC1 inhibitors abrogate this feedback suppression, resulting in Akt activation. Indeed, Cloughesy and colleagues (39) reported that rapamycin treatment induces an increase in phosphorylation of Akt in a subset of patients with phosphatase and tension homolog (PTEN)-deficient glioblastoma. Therefore, the use of mTORC1 inhibitors risks the possible activation of Akt by disruption of a negative

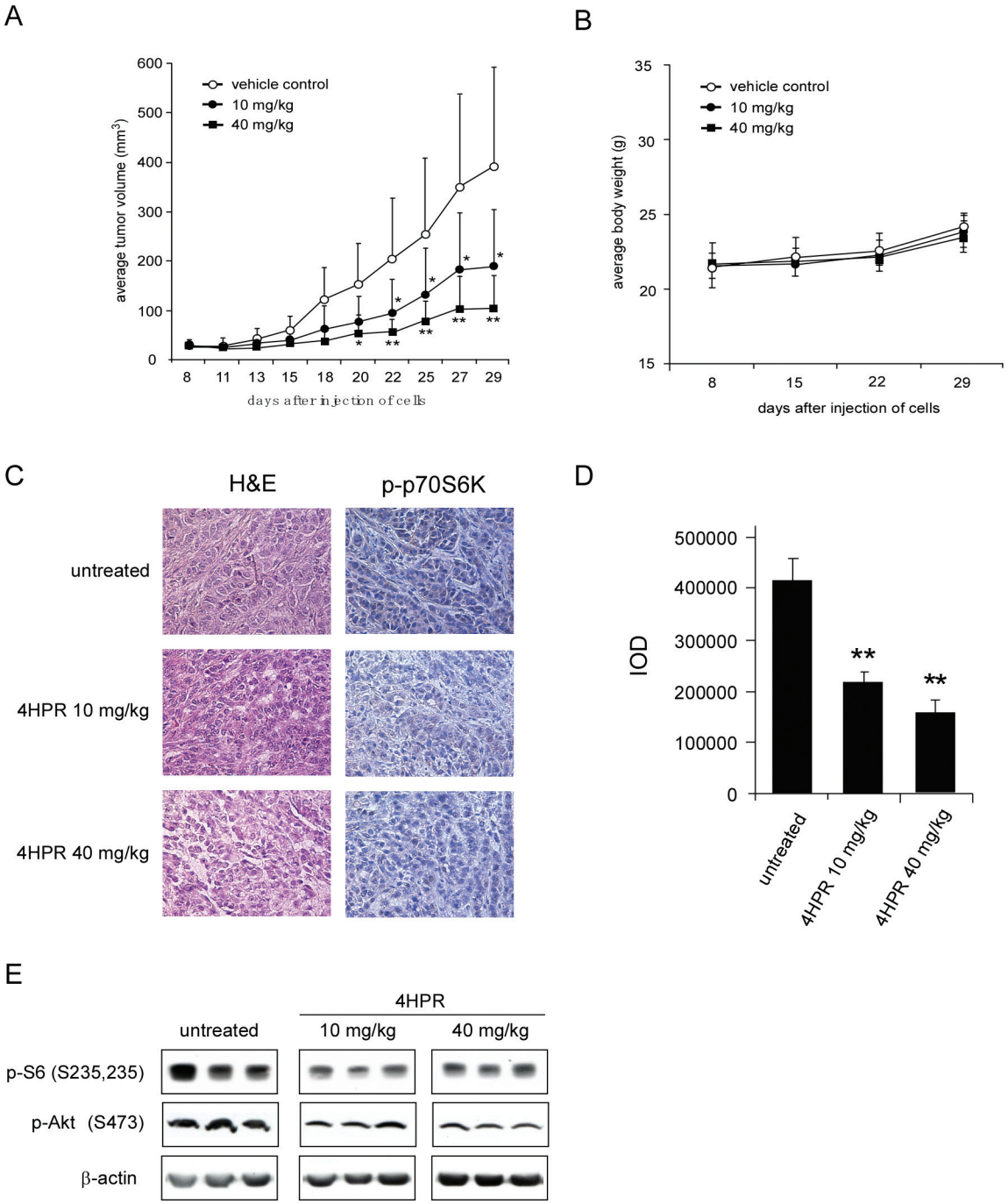

Fig. 6. Effect of 4HPR on lung cancer growth and mTOR targets in an A549 xenograft mouse model. (**A**) 4HPR significantly suppresses lung cancer cell growth. The average tumor volume of vehicle-treated control mice and 4HPR-treated mice plotted over 29 days after tumor cell injection. Data are shown as means ±standard error of measurements. The *P* values indicate a significant inhibition by 4HPR on tumor growth (*$P < 0.05$; **$P < 0.01$). (**B**) 4HPR has no effect on mouse body weight. Body weights from treated or untreated groups of mice were measured once a week. (**C**) H&E staining and immunohistochemical analysis of tumor tissues. Treated or untreated groups of mice were euthanized and tumors extracted. Lung cancer tissue slides were prepared with paraffin sections after fixation with formalin and then stained with H&E or antiphospho-p70S6K (T389). (**D**) quantification of expression of phospho-p70S6K (T389) in tumor tissues using the Image-Pro Plus software program and data are shown as integrated optical density units. (**E**) 4HPR inhibits mTOR-targeted protein expression in A549 lung cancer tissues. The tumor tissues from groups treated with vehicle, 10 mg 4HPR/kg body weight (B.W.), or 40 mg 4HPR/kg B.W. were immunoblotted with antibodies to detect phosphorylated S6 (S235, S236). Expression of β-actin was used to verify equal protein loading.

feedback loop, and patients treated with these drugs eventually become refractory. In the present study, we demonstrated that 4HPR was able to inhibit the binding of mTOR with both rictor of mTORC2 and raptor of mTORC1, suggesting its ability to silence the rictor-dependent positive feedback loop on Akt activation. Consistent with this point, our results confirmed that 4HPR can inhibit the phosphorylation of Akt (Ser473) at a dose that suppressed the phosphorylation of both p70S6K and S6, in different types of lung cancer cell lines. In contrast, rictor

downregulation was not achieved in A549 cells treated with rapamycin at a concentration that can dramatically inhibit p70S6K phosphorylation and S6 phosphorylation, which is consistent with previous reports. These data provide strong evidence that 4HPR is an effective inhibitor that targets both mTORC1 and mTORC2, possessing an advantage over rapalogues in Akt inhibition.

Taken together, the results of present study identify mTOR as a direct and important target of 4HPR, which offers useful evidence for the rational use and combinational treatment of 4HPR in cancer therapy. Meanwhile, we cannot exclude the possibility that 4HPR treatment, besides decreasing mTOR activity, leads to antitumor activity by affecting other pathways, which have been reported previously by several groups (5,11–13,15). Moreover, in order to further validate the functional role of the binding between 4HPR and mTOR, experiments utilizing overexpression of wild type and mTOR mutant cancer cells will be performed in the near future. Numerous preclinical studies and clinical trials of 4HPR are still ongoing in different countries (1), and more work needs to be performed in the future to provide more valuable evidence for guiding the clinical use of 4HPR in cancer prevention and therapy (34).

Funding

The Hormel Foundation and National Institutes of Health (CA027502, CA120388, R37 CA081064 and ES016548) and NCI Contract Number HHSN-261200533001C-NO1-CN-53301 and N01-CN-43309-18018-01WA 13B.

Acknowledgements

We would like to thank Tonya Poorman for her help in submitting our manuscript.

References

1. Sogno,I. *et al.* (2010) Angioprevention with fenretinide: targeting angiogenesis in prevention and therapeutic strategies. *Crit. Rev. Oncol. Hematol.*, **75**, 2–14.
2. Abou-Issa,H. *et al.* (1995) Relative efficacy of glucarate on the initiation and promotion phases of rat mammary carcinogenesis. *Anticancer Res.*, **15**, 805–810.
3. Decensi,A. *et al.* (1994) Pilot study of high dose fenretinide and vitamin A supplementation in bladder cancer. *Eur. J. Cancer*, **30A**, 1909–1910.
4. Zhu,G. *et al.* (2007) Polymeric retinoid prodrug PG-4HPR enhances the radiation response of lung cancer. *Oncol. Rep.*, **18**, 645–651.
5. Benelli,R. *et al.* (2010) The chemopreventive retinoid 4HPR impairs prostate cancer cell migration and invasion by interfering with FAK/AKT/GSK3beta pathway and beta-catenin stability. *Mol. Cancer*, **9**, 142.
6. Lai,W.L. *et al.* (2008) The PERK/eIF2 alpha signaling pathway of unfolded protein response is essential for N-(4-hydroxyphenyl)retinamide (4HPR)-induced cytotoxicity in cancer cells. *Exp. Cell Res.*, **314**, 1667–1682.
7. DiPietrantonio,A.M. *et al.* (1998) Regulation of G1/S transition and induction of apoptosis in HL-60 leukemia cells by fenretinide (4HPR). *Int. J. Cancer*, **78**, 53–61.
8. Veronesi,U. *et al.* (1999) Randomized trial of fenretinide to prevent second breast malignancy in women with early breast cancer. *J. Natl. Cancer Inst.*, **91**, 1847–1456.
9. Sabichi,A.L. *et al.* (1998) Retinoic acid receptor beta expression and growth inhibition of gynecologic cancer cells by the synthetic retinoid N-(4-hydroxyphenyl) retinamide. *J. Natl. Cancer Inst.*, **90**, 597–605.
10. Lovat,P.E. *et al.* (2000) Effector mechanisms of fenretinide-induced apoptosis in neuroblastoma. *Exp. Cell Res.*, **260**, 50–60.
11. Sun,S.Y. *et al.* (1999) Mediation of N-(4-hydoxyphenyl)retinamide-induced apoptosis in human cancer cells by different mechanisms. *Cancer Res.*, **59**, 2493–2498.
12. Chen,Y.R. *et al.* (1999) c-Jun N-terminal kinase mediates apoptotic signaling induced by N-(4-hydroxyphenyl)retinamide. *Mol. Pharmacol.*, **56**, 1271–1279.
13. Kini,A.R., *et al.* (2001) Angiogenesis in acute promyelocytic leukemia: induction by vascular endothelial growth factor and inhibition by all-trans retinoic acid. *Blood*, **97**, 3919–3924.
14. Pili,R., *et al.* (2001) Combination of phenylbutyrate and 13-cis retinoic acid inhibits prostate tumor growth and angiogenesis. *Cancer Res.*, **61**, 1477–1485.
15. Kim,J.H. *et al.* (1995) In vitro anti-invasive effects of N-(4-hydroxyphenyl)-retinamide on human prostatic adenocarcinoma. *Anticancer Res.*, **15**, 1429–1434.
16. Simeone,A.M., *et al.* (2006) N-(4-Hydroxyphenyl)retinamide and nitric oxide pro-drugs exhibit apoptotic and anti-invasive effects against bone metastatic breast cancer cells. *Carcinogenesis*, **27**, 568–577.
17. Cao,J., *et al.* (2009) ROS-driven Akt dephosphorylation at Ser-473 is involved in 4-HPR-mediated apoptosis in NB4 cells. *Free Radic. Biol. Med.*, **47**, 536–547.
18. Rahmaniyan,M. *et al.* (2011) Identification of dihydroceramide desaturase as a direct in vitro target for fenretinide. *J. Biol. Chem.*, **286**, 24754–24764.
19. Guertin,D.A. *et al.* (2007) Defining the role of mTOR in cancer. *Cancer Cell*, **12**, 9–22.
20. Hsu,P.P. *et al.* (2011) The mTOR-regulated phosphoproteome reveals a mechanism of mTORC1-mediated inhibition of growth factor signaling. *Science*, **332**, 1317–1322.
21. Sarbassov,D.D. *et al.* (2005) Phosphorylation and regulation of Akt/PKB by the rictor-mTOR complex. *Science*, **307**, 1098–1101.
22. Liu,P. *et al.* (2009) Targeting the phosphoinositide 3-kinase pathway in cancer. *Nat. Rev. Drug Discov.*, **8**, 627–644.
23. Choi,J. *et al.* (1996) Structure of the FKBP12-rapamycin complex interacting with the binding domain of human FRAP. *Science*, **273**, 239–242.
24. Yu,K. *et al.* (2010) Beyond rapalog therapy: preclinical pharmacology and antitumor activity of WYE-125132, an ATP-competitive and specific inhibitor of mTORC1 and mTORC2. *Cancer Res.*, **70**, 621–631.
25. Wang,X. *et al.* (2008) Enhancing mammalian target of rapamycin (mTOR)-targeted cancer therapy by preventing mTOR/raptor inhibition-initiated, mTOR/rictor-independent Akt activation. *Cancer Res.*, **68**, 7409–7418.
26. Gopal,A.K. *et al.* (2004) Fenretinide enhances rituximab-induced cytotoxicity against B-cell lymphoma xenografts through a caspase-dependent mechanism. *Blood*, **103**, 3516–3520.
27. Formelli,F. *et al.* (2000) Therapeutic effects of the combination of fenretinide and all-trans-retinoic acid and of the two retinoids with cisplatin in a human ovarian carcinoma xenograft and in a cisplatin-resistant sub-line. *Eur. J. Cancer*, **36**, 2411–2419.
28. Freedman,V.H. *et al.* (1974) Cellular tumorigenicity in nude mice: correlation with cell growth in semi-solid medium. *Cell*, **3**, 355–359.
29. Kiefer,F. *et al.* (2009) The SWISS-MODEL Repository and associated resources. *Nucleic Acids Res.*, **37**, D387–D392.
30. Berndt,A. *et al.* (2010) The p110 delta structure: mechanisms for selectivity and potency of new PI(3)K inhibitors. *Nat. Chem. Biol.*, **6**, 117–124.
31. Gately,K. *et al.* (2012) Overexpression of the mammalian target of rapamycin (mTOR) and angioinvasion are poor prognostic factors in early stage NSCLC: a verification study. *Lung Cancer*, **75**, 217–222.
32. Dobashi,Y., *et al.* (2009) Critical and diverse involvement of Akt/mammalian target of rapamycin signaling in human lung carcinomas. *Cancer*, **115**, 107–118.
33. Dobashi,Y. *et al.* (2011) Paradigm of kinase-driven pathway downstream of epidermal growth factor receptor/Akt in human lung carcinomas. *Hum. Pathol.*, **42**, 214–226.
34. McDonald,J.M. *et al.* (2008) Elevated phospho-S6 expression is associated with metastasis in adenocarcinoma of the lung. *Clin. Cancer Res.*, **14**, 7832–7837.
35. Formelli,F. *et al.* (2008) Pharmacokinetics of oral fenretinide in neuroblastoma patients: indications for optimal dose and dosing schedule also with respect to the active metabolite 4-oxo-fenretinide. *Cancer Chemother. Pharmacol.*, **62**, 655–665.
36. Wang,L. *et al.* (2009) Mammalian target of rapamycin complex 1 (mTORC1) activity is associated with phosphorylation of raptor by mTOR. *J. Biol. Chem.*, **284**, 14693–14697.
37. Tobak,A. *et al.* (2007) Construction of the 3D structure of the mTOR kinase-domain and discovery of novel mTOR inhibitors. PhD thesis, Rutgers University.
38. Buck,E. *et al.* (2008) Feedback mechanisms promote cooperativity for small molecule inhibitors of epidermal and insulin-like growth factor receptors. *Cancer Res.*, **68**, 8322–8332.
39. Cloughesy,T.F. *et al.* (2008) Antitumor activity of rapamycin in a Phase I trial for patients with recurrent PTEN-deficient glioblastoma. *PLoS Med.*, **5**, e8.

Received April 23, 2012; revised June 28, 2012; accepted July 8, 2012